An energy landscape approach to locomotor transitions in complex 3D terrain

Ratan Othayoth[a], George Thoms[a], and Chen Li[a,1]

[a]Department of Mechanical Engineering, Johns Hopkins University, Baltimore, MD 21218

Edited by David A. Weitz, Harvard University, Cambridge, MA, and approved May 6, 2020 (received for review October 18, 2019)

Effective locomotion in nature happens by transitioning across multiple modes (e.g., walk, run, climb). Despite this, far more mechanistic understanding of terrestrial locomotion has been on how to generate and stabilize around near–steady-state movement in a single mode. We still know little about how locomotor transitions emerge from physical interaction with complex terrain. Consequently, robots largely rely on geometric maps to avoid obstacles, not traverse them. Recent studies revealed that locomotor transitions in complex three-dimensional (3D) terrain occur probabilistically via multiple pathways. Here, we show that an energy landscape approach elucidates the underlying physical principles. We discovered that locomotor transitions of animals and robots self-propelled through complex 3D terrain correspond to barrier-crossing transitions on a potential energy landscape. Locomotor modes are attracted to landscape basins separated by potential energy barriers. Kinetic energy fluctuation from oscillatory self-propulsion helps the system stochastically escape from one basin and reach another to make transitions. Escape is more likely toward lower barrier direction. These principles are surprisingly similar to those of near-equilibrium, microscopic systems. Analogous to free-energy landscapes for multipathway protein folding transitions, our energy landscape approach from first principles is the beginning of a statistical physics theory of multipathway locomotor transitions in complex terrain. This will not only help understand how the organization of animal behavior emerges from multiscale interactions between their neural and mechanical systems and the physical environment, but also guide robot design, control, and planning over the large, intractable locomotor-terrain parameter space to generate robust locomotor transitions through the real world.

locomotion | obstacle traversal | potential energy barrier | kinetic energy fluctuation | terradynamics

To move about in the environment, animals can use many modes* of locomotion (e.g., walk, run, crawl, climb, fly, swim, jump, burrow) (1–3) and must often transition across them (4, 5) (e.g., Fig. 1*A* and Movie S1). Despite this, far more of our mechanistic understanding of terrestrial locomotion has been on how animals generate (6–10) and stabilize (11–14) steady-state, limit-cycle–like locomotion using a single mode.

Recent studies begin to reveal how terrestrial animals transition across locomotor modes in complex environments. Locomotor transitions, like other animal behavior, emerge from multiscale interactions of the animal and external environment across the neural, postural, navigational, and ecological levels (15–17). At the neural level, terrestrial animals can use central pattern generators (18) and sensory information (19–21) to switch locomotor modes to traverse different media or overcome obstacles. At the ecological level, terrestrial animals foraging across natural landscapes switch locomotor modes to minimize metabolic cost (22). At the intermediate level, terrestrial animals also transition between walking and running to save energy (23). However, there remains a knowledge gap in how locomotor transitions in complex terrain emerge from direct physical interaction [i.e., terradynamics (24)] of an animal's body and appendages with the environment. In particular, we lack theoretical concepts for thinking about how to generate and control locomotor transitions in complex terrain that are on the same level of limit cycles for single-mode locomotion (25). For example, locomotion in irregular terrain with repeated perturbations is rarely near steady state and requires an animal to continually modify its behavior, which cannot be well described by limit cycles (26, 27).

Understanding of how to make use of physical interaction with complex terrain [environmental affordance (28, 29)] to generate and control locomotor transitions is also critical to advancing mobile robotics. Similar to personal computers decades ago, mobile robots are on the verge of becoming a part of society. Some robots (e.g., robot vacuums, self-driving cars) already excel at navigating flat surfaces, by transitioning across driving modes [e.g., forward drive, U-turn, stop, park (30)] to avoid sparse obstacles using a geometric map of the environment (31). However, many critical applications, such as search and rescue in rubble, inspection and monitoring in buildings, extraterrestrial exploration through rocks, and even drug delivery inside a human body, require robots to transition across diverse locomotor modes to traverse unavoidable obstacles in complex terrain (4, 5, 32) (Fig. 1*B*). However, terrestrial robots still struggle to do so robustly (33), because we do not understand well how locomotor transitions (or lack thereof) emerge from physical interaction with complex terrain.

Significance

Effective locomotion in nature happens by transitioning across multiple modes (e.g., walk, run, climb). Using laboratory experiments on a model system, we demonstrate that an energy landscape approach helps understand how multipathway transitions across locomotor modes in complex 3D terrain statistically emerge from physical interaction. Animals' and robots' locomotor modes are attracted to basins of a potential energy landscape. They can use kinetic energy fluctuation from oscillatory self-propulsion to cross potential energy barriers, escaping from one basin and reaching another to make locomotor transitions. Our first-principle energy landscape approach is the beginning of a statistical physics theory of locomotor transitions in complex terrain. It will help understand and predict how animals, and how robots should, move through the real world.

Author contributions: R.O. and C.L. designed research; R.O. performed research; G.T. contributed new experimental tools; R.O. analyzed data; and R.O. and C.L. wrote the paper.

The authors declare no competing interest.

This article is a PNAS Direct Submission.

[1]To whom correspondence may be addressed. Email: chen.li@jhu.edu.

This article contains supporting information online at https://www.pnas.org/lookup/suppl/doi:10.1073/pnas.1918297117/-/DCSupplemental.

First published June 15, 2020.

*Here, we use mode in the general sense to refer to distinct, stereotyped locomotor behavior, not confined to limit-cycle behavior such as gaits or templates (25).

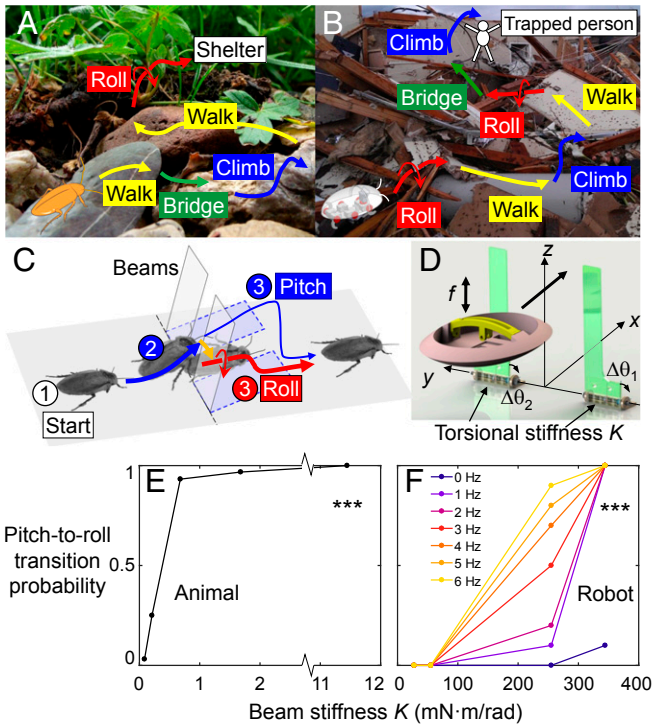

Fig. 1. Locomotor transitions of animals and robots in complex terrain. (*A* and *B*) Illustrative locomotor transitions of (*A*) a cockroach traversing forest floor (image credit: Scott Brill [photographer]) and (*B*) a robot traversing rubble for search and rescue. (*C*) A cockroach transitioning (orange arrow) from pitch to roll mode to traverse grass-like beam obstacles. (*D*) Robotic physical model. (*E* and *F*) Pitch-to-roll transition probability of animal (*E*) and robot (*F*) as a function of beam stiffness *K*. For robot, we varied oscillation frequency *f* to vary kinetic energy fluctuation. ***Significant dependence on *K* (animal: mixed-effects χ^2 test, $P < 0.0001$, $\chi^2 = 297.4$; robot: χ^2 test, $P < 0.0001$, $\chi^2 = 247.1$). $n = 64$, 60, 60, 62, and 64 trials for animal and $n = 70$ trials at each *K* for robot. Note that at $f = 0$, transition occurred in one trial at $K = 344$ mN·m/rad (resulting in a 10% probability) due to lateral displacement of the body. This was from lateral bending of the vertical bar driving the body forward due to large lateral force from the stiff beams, an effect not captured by our model.

Our study is motivated by recent observations in a model system of insects traversing complex three-dimensional (3D) terrain. The discoid cockroach, native to rainforest floor, can traverse flexible, grass-like beam obstacles using many locomotor modes, stochastically transitioning across them via multiple pathways (34). For simplicity, hereafter we focus on the transition between two modes. The animal often first pushes against the beams, and beam elastic restoring forces lead the animal body to pitch up (Fig. 1*C*, blue). After this, however, the animal rarely pushes across (3% probability) but often rolls (Fig. 1*C*, red) to maneuver through beam gaps (45% probability). We define these as "pitch" and "roll" modes. Note that we use "locomotor mode" here in the general sense, not confined to limit-cycle locomotor behavior. The pitch mode is more challenging than the roll mode because the animal has to lift its weight and deflect the beams more (this is only true when beams are stiff, however; see *Results*). Thus, the animal appears to statistically transition from less to more favorable modes. In addition, the animal's body oscillates as its legs continually pushed against the ground when trying to traverse. Besides in obstacle traversal, similar multipathway locomotor transitions, preference of some modes over others, and seemingly wasteful body oscillation were observed in self-righting of insects (35).

In the field of protein folding, adopting a statistical physics view and using an energy landscape approach led researchers to recognize that proteins fold via multiple pathways and understand the physical principles (36–38). These near-equilibrium, microscopic systems statistically transition from higher to lower energy states (local minima) on a free-energy landscape (increasing thermodynamic favorability). Thermal fluctuation helps the system stochastically cross energy barriers at transition states (saddle points between local minimum basins). These physical principles operating on a rugged landscape lead to the multipathway protein folding transitions. Inspired by the seeming similarities of our system to them, we contend that an energy landscape approach helps understand how self-propelled, far-from-equilibrium macroscopic animals' and robots' probabilistic locomotor transitions in complex 3D terrain emerge from physical interaction, whose equations of motion are unknown or intractable (39, 40). Specifically, we hypothesize that 1) the self-propelled system's state is attracted to a local minimum basin on a potential energy landscape; locomotor transition from one mode to another can be viewed as the system state escaping from one basin and settling into another. (What governs transition?) 2) When it is comparable to the potential barrier, kinetic energy fluctuation from oscillatory self-propulsion helps the system escape from a landscape basin to make locomotor transitions. (When does transition happen?) 3) Escape from a basin is more likely toward a direction along which the escape barrier is lower. (How does transition happen?)

To begin to establish an energy landscape approach of locomotor transitions across modes in complex 3D terrain, we tested these hypotheses for the two representative modes (pitch and roll) of the model body–beam interaction system defined above. Although the previous study introduced an early energy landscape model to qualitatively explain why locomotor shape affected physical interaction and thus locomotion (34), none of these hypotheses were proposed or tested. We emphasize that our potential energy landscape directly arises from locomotor-terrain interaction physics using first principles. This is unlike artificially defined potential functions to explain walk-to-run transition (41) and other nonequilibrium biological phase transitions (42), or metabolic energy landscapes inferred from oxygen consumption measurements to explain behavioral switching of locomotor modes (22).

Because animal locomotion emerges from complex interactions of neural and physical mechanisms (1), to observe the outcome of pure physical interaction, we developed and tested a minimalistic robotic physical model (Fig. 1*D* and Movie S2) with feedforward control. The robot had an ellipsoid-like body that was propelled forward at a constant speed and was free to pitch and roll (achieved through a gyroscope mechanism) in response to interaction with two beams. The body was constrained not to yaw or move laterally to simplify energy landscape modeling. We also performed experiments with the discoid cockroach traversing beams during escape response to study how physical interaction affects the animal's locomotor transitions when neural control is bandwidth limited (1). Comparison of robot and animal observations can reveal aspects of the transitions that likely involve neural mechanisms.

To test the first hypothesis, in both robot and animal experiments, we used rigid "beams" with torsional joints at the base (*SI Appendix*, Figs. S1 and S2) as one-degree-of-freedom 3D terrain components to generate a simple potential energy landscape. We then calculated the potential energy landscape and 3D motion of the robot or animal body and beams in high accuracy [as opposed to visual examination in the previous study (34)] (*SI Appendix*, Figs. S3 and S4 and Movies S3 and S4) for the entire traversal. This allowed us to quantify how the system state behaved on the landscape during each observed locomotor mode and transition between modes. To test the second hypothesis, for the robot, we

applied controlled oscillation with variable frequency f to vary kinetic energy fluctuation (*SI Appendix*, Fig. S5). Because we could not vary the animal's naturally occurring body oscillation, in animal experiments we changed the barrier relative to kinetic energy oscillation by varying beam torsional joint stiffness K by over an order of magnitude in the range of natural flexible terrain elements (*SI Appendix*, Table S2). K was also varied by over an order of magnitude for robot experiments and, together with animal experiments, helped elucidate how transition depended on terrain properties. Because the potential energy landscape consists of not only beam elastic energy but also body and beam gravitational energy, variation of K also changed how escape barrier compared in different directions, allowing the third hypothesis to be tested. See *Methods* and *SI Appendix*, *Supplementary Methods* for technical detail and *SI Appendix*, Table S1 for sample sizes.

Results

Before encountering the beams, both the robot and animal moved forward with a near horizontal body posture. After beam contact, both the robot and animal started traversing by pushing against the beams, with the body pitched up. As beam stiffness K increased, pitch-to-roll transition probability increased for both the robot and animal (Fig. 1 *E* and *F*; $P < 0.0001$, mixed-design χ^2 test). At low K, neither transitioned to the roll mode even with body oscillation. At the highest K, both always transitioned, except for the robot without oscillation. In addition, for the robot at high K (255 mN·m/rad), pitch-to-roll transition probability increased with oscillation frequency f (Fig. 1*F*) and thus with kinetic energy fluctuation (*SI Appendix*, Fig. S5*A*). At the highest K tested (344 mN·m/rad), pitch-to-roll transition probability reached 1 for all $f > 0$ tested. For simplicity, below we first describe robot results followed by animal results.

We tested the first hypothesis by calculating the robot's potential energy landscape and evaluating how its system state behaved on the landscape (Fig. 2 and Movie S4). Using the measured physical and geometric parameters of the body and beams, we calculated the robot's system potential energy (sum of body and beam gravitational energy and beam elastic energy) as a function of body pitch, roll, and forward position x relative to the beams. For simplicity, we first examine results at $K = 255$ N·m/rad. Before the body contacted the beams (Fig. 2 *A*, *i*), pitching or rolling increased body gravitational energy (because body center of mass was below rotation axes; *SI Appendix*, Fig. S6). Thus, the potential energy landscape over body pitch–roll space had a global minimum at zero pitch and zero roll, i.e., when the body was horizontal (Fig. 2 *B*, *i*). As the body moved closer and interacted with the beams (Fig. 2 *A*, *ii* and *iii*), the global minimum evolved into a "pitch" local minimum at a finite pitch and zero roll (Fig. 2 *B*, *ii* and *iii*, blue). Meanwhile, two "roll" local minima emerged at near zero pitch and a finite positive or negative roll (Fig. 2 *B*, *ii* and *iii*, red, for rolling right

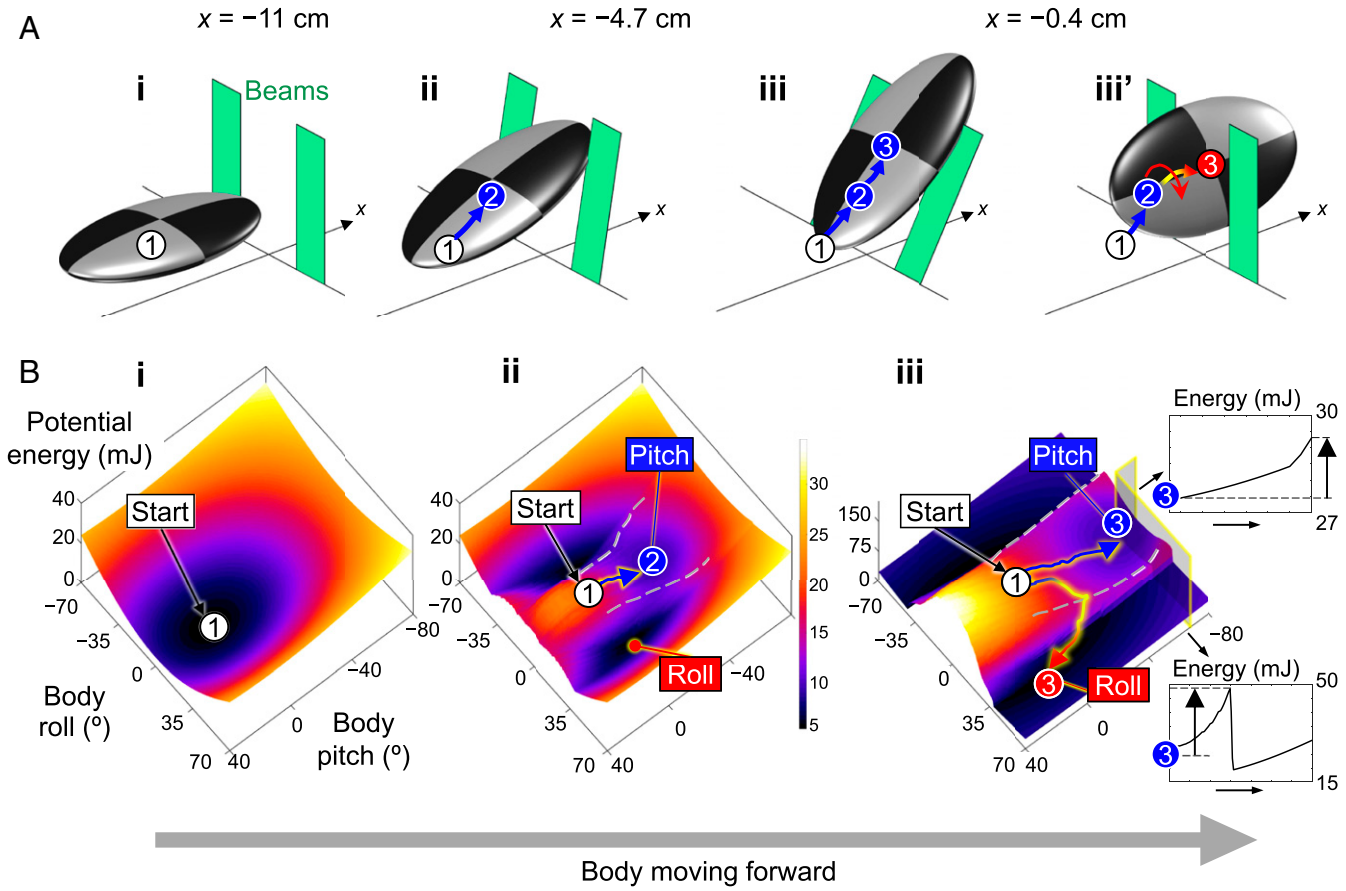

Fig. 2. Robot locomotor transitions on a potential energy landscape. Results are shown at $K = 255$ mN·m/rad. (*A*) Snapshots of body before and during interaction with two beams in pitch (*i*, *ii*, and *iii*) and roll (*iii'*) modes. (*B*) Snapshots of landscape over body pitch–roll space before (*i*) and during (*ii* and *iii*) interaction. Representative system state trajectories are shown for being trapped in pitch basin (blue) and transitioning to roll basin (red). Insets in *iii* define potential energy barriers to escape from pitch local minimum in pitch-up and positive roll directions. The dashed gray curves on landscape show boundaries between pitch and roll basins. Note that landscape evolves as body moves forward (increasing x), and only part of landscape over pitch–roll space is shown to focus on pitch and roll basins.

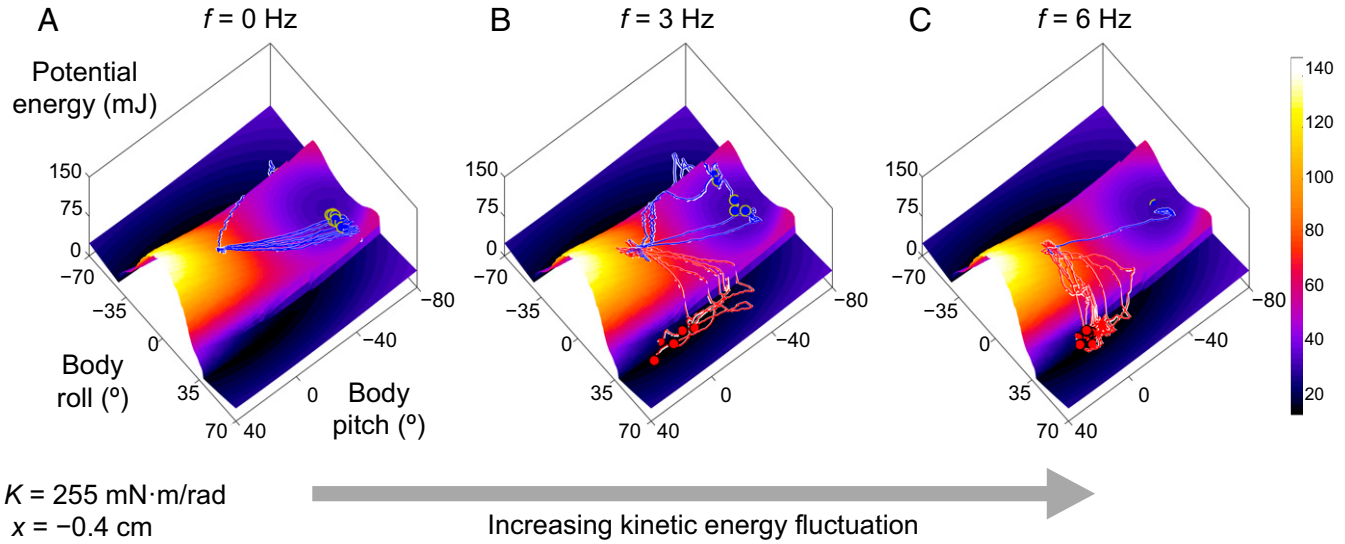

Fig. 3. Robot locomotor transitions are stochastic and become more likely as kinetic energy fluctuation increases. Comparison of state trajectory ensemble on average landscape (snapshot at $x = -0.4$ cm) across oscillation frequencies: (*A*) $f = 0$ Hz; (*B*) $f = 3$ Hz; and (*C*) $f = 6$ Hz. Results are shown at $K = 255$ mN·m/rad. The blue and red curves show trials trapped in pitch basin and transitioning to roll basin, respectively. Trials in which body rolls left are flipped to rolling right considering lateral symmetry. $n = 10$ trials at each f. Only part of landscape over pitch–roll space is shown to focus on pitch and roll basins. Blue trajectories exiting pitch basin are an artifact of landscape averaging.

or left), whose energies were lower than the pitch local minimum. Hereafter, we refer to these local minimum basins as pitch and roll basins.†

We discovered that the robot's system state during the observed pitch and roll modes were attracted to the pitch and roll basins, respectively. When the body was far away from the beams, the system state in pitch and roll space settled to the global minimum of the landscape (Fig. 2 *B*, *i* and Movie S4). During beam interaction, without oscillation, the system state was trapped in the pitch basin, leading to the body pushing across the beams in a pitched-up orientation with little roll (Fig. 2 *A* and *B*, *ii* and *iii*, and Movie S4, *Top*). With oscillation, the system stochastically escaped from the pitch basin and crossed a potential energy barrier to reach the roll basin (Fig. 2 *B*, *iii*, and Movie S4, *Bottom*), thereby transitioning from the pitch to the roll mode (Fig. 2 *B*, *ii* and *iii′*). We examined system state trajectory on the landscape calculated for each trial (see examples in Movie S6, third row). Whether the robot was trapped in the pitch mode (blue trajectories) or transitioned to the roll mode (red trajectories), its system state was attracted to the corresponding basin in nearly all trials (99%, not significantly different from 1, $P > 0.15$, Student's t test; see Fig. 4 *A*, *iii*). Because of this strong attraction, the measured system potential energy closely matched the observed mode basin's local minimum energy throughout traversal (see Fig. 5, *iii*, solid vs. dashed curves). All of these findings held true at other K (near 100%; see Figs. 4*A* and 5, and Movie S6). Together, these robot results supported our first hypothesis.

Next, we tested the second hypothesis. We first observed how kinetic energy fluctuation affected the robot's escape from a basin. Again, we examine results at $K = 255$ N·m/rad first for simplicity. As f increased (which increased kinetic energy fluctuation), the system was more likely to escape from the pitch basin it was initially attracted to and reach the roll basin (Fig. 3 and Movie S5), resulting in more likely pitch-to-roll transitions (Fig. 1*F*; $K = 255$ mN·m/rad). Then, we compared the minimal potential energy barrier to escape from the pitch local minimum with the average kinetic energy fluctuation at $f = 6$ Hz (Fig. 4 *C*, *iii*, and Movie S7, *Bottom*). The escape barrier depended on both toward which direction the system moved in the pitch–roll space (Fig. 2 *B*, *iii* and *Insets*, and Fig. 4 *B*, *iii*) and body forward position x relative to the beams (Fig. 4 *C*, *iii*, and Movie S7, *Bottom*). Minimal escape barrier occurred at the saddle point between the pitch and roll basins (Fig. 4*C*, yellow dot), which we defined as pitch-to-roll transition barrier. Only within a small range of x was average kinetic energy fluctuation at $f = 6$ Hz (Fig. 4 *C*, *iii*, green) sufficient for overcoming pitch-to-roll transition barrier (Fig. 4 *C*, *iii*, black, and Movie S8, third column). This range matched remarkably well with the x range over which pitch-to-roll transition was observed with increasing likelihood with f (gray band showing mean ± SD from all trials across f). All these findings held true at $K = 344$ N·m/rad. At $K = 28$ N·m/rad, minimal escape barrier far exceeded kinetic energy fluctuation, consistent with the absence of transition. Together, these robot results supported our second hypothesis.

Finally, we tested the third hypothesis by examining the direction toward which the robot's system state moved during interaction. At each K, when the body was not in contact with the beams, the escape barrier was large along all directions in the pitch–roll space (Movie S7, *Bottom*, and Movie S8, second row; e.g., $x = -80$ mm). As the body moved forward (increasing x), the escape barrier toward the direction of roll basins reduced drastically, becoming comparable to or even smaller than average kinetic energy fluctuation at $f = 6$ Hz (green circle) at the saddle point (yellow dot). By contrast, escape barrier in the direction of pitching up or down was always greater than average kinetic energy fluctuation (Fig. 4*B* and Movie S8, third row). Examination of how the system state moved on the landscape (Movie S9, *Top*) and probability distribution of system state velocity directions in the pitch–roll space (Fig. 4*D* and Movie S9, *Bottom*) showed that escape was more aligned with the direction of the saddle point between pitch and roll basins, i.e., escape was more likely toward the direction of lower barrier. This is intuitive because in other directions escape barrier was higher and often

†A fourth basin also emerged with its local minimum at a finite positive pitch and zero roll, corresponding to the body pitching down against the beams. However, such a configuration was never observed in the robot or animal.

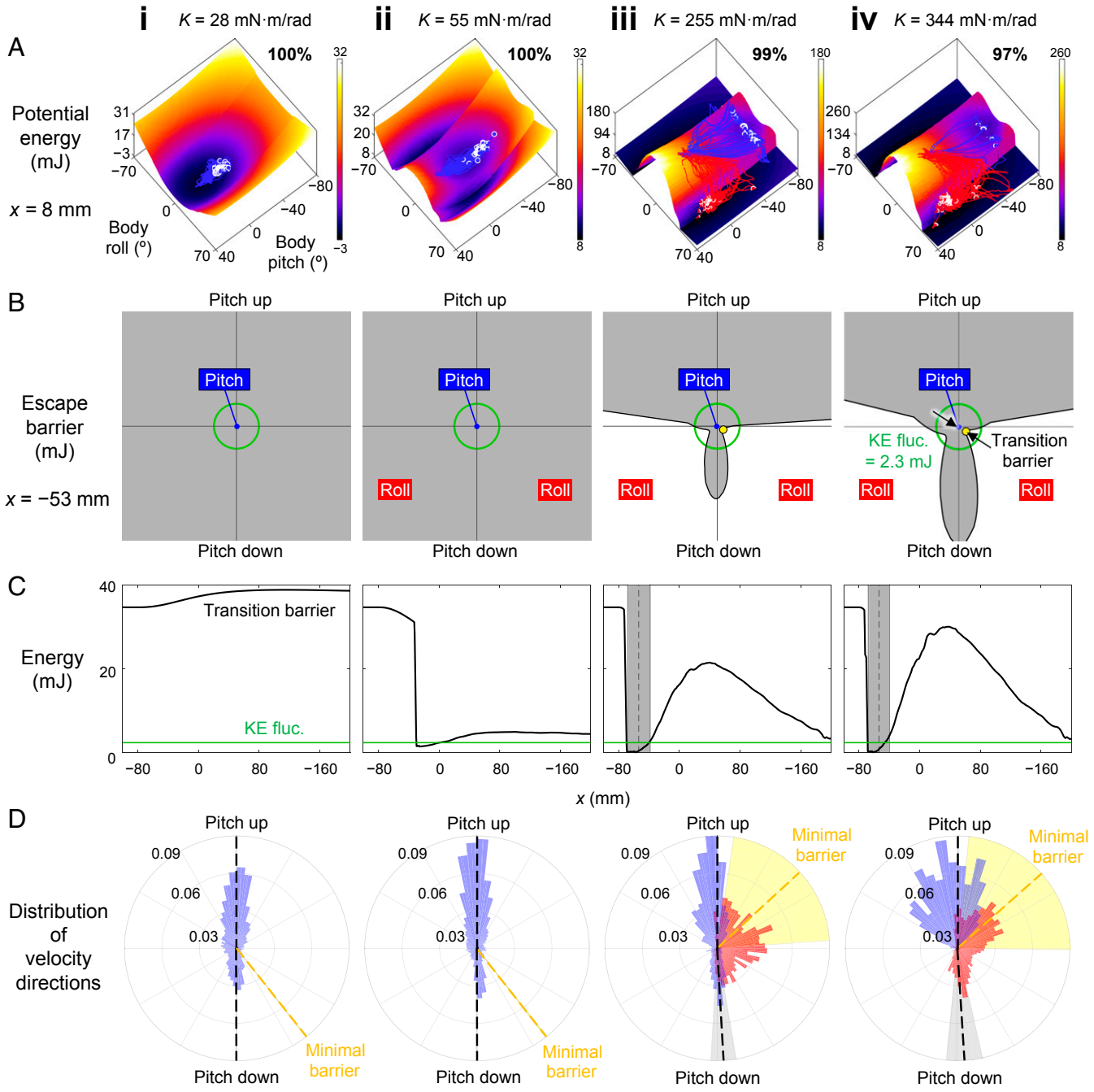

Fig. 4. Robot tends to transition to roll basin when kinetic energy fluctuation is comparable to potential energy barrier to escape pitch local minimum and toward direction of lower barrier. (*A*) Average potential energy landscape over pitch–roll space (snapshot at $x = 8$ mm) with ensemble of state trajectories. The blue and red curves show trials trapped in pitch basin and transitioning to roll basin, respectively. Note that landscape evolves as body moves forward (increasing x) (Movie S8), and only part of the landscape over pitch–roll space is shown to focus on the pitch and roll basins. Top right number on each landscape shows percentage of trials in which system state is attracted to pitch/roll basin corresponding to observed mode. The blue trajectories exiting pitch basin are an artifact of landscape averaging. (*B*) Polar plot of potential energy barrier to escape from pitch local minimum (blue dot) along all directions in pitch–roll space (snapshot at $x = -53$ mm). Pitch-to-roll transition barrier is defined as minimal escape barrier (arrows in *iv*), which occurs at saddle point between pitch and roll basins (yellow dot). (*C*) Pitch-to-roll transition barrier as a function of x. The gray band shows x range in which pitch-to-roll transition is observed (mean ± SD). The green circle/line in *B* and *D* shows measured average kinetic energy fluctuation of 2.3 mJ at highest $f = 6$ Hz tested (*SI Appendix*, Fig. S5*A*). (*D*) Probability distribution of state velocity directions in pitch–roll space in the x range where transition is observed (gray band in *C*). Blue and red are data from trials trapped in pitch basin and transitioning to roll basin, respectively. Trials in which body rolls left are flipped to rolling right considering lateral symmetry. The black dashed lines and gray shaded sectors show angular direction of maximal escape barriers (mean ± SD) along pitch up and down directions. The yellow dashed line and shaded sector show angular direction of minimal escape barrier (mean ± SD), which occurs at saddle point. Columns *i*–*iv* are at $K = 28$, 55, 255, and 344 mN·m/rad. Data shown in *A*, *C*, and *D* are for all f tested ($n = 70$ trials) at each K.

exceeded kinetic energy fluctuation. Together, these robot observations supported our third hypothesis.

Comparison of robot observations across K further suggested a concept of favorability for locomotor transitions. As K increased, pitch-to-roll transition became more likely (Fig. 4*A*), saturating at 1 for all $f > 0$ tested at the highest K (Fig. 1*F*). Intuitively, when the beams were flimsy, the body pushed across (trapped in the pitch mode) as if nothing were there; when the beams were rigid, the body could not push across and must roll. Thus, the likelihood of pitch-to-roll transition is positively correlated with how favorable transitioning to the roll mode is relative to staying in the pitch mode. To provide a measure of favorability, we compared whether the pitch or roll basin was lower during traversal, measured at their respective local minimum (Fig. 5 and Movie S8, fourth row). At low K (28 mN·m/rad), the pitch basin remained the global minimum basin throughout traversal (Fig. 5, *i*), indicating that the pitch mode was more favorable. As K increased, the pitch basin became increasingly higher than the roll basin (Fig. 5, *ii*–iv), indicating that the roll mode became increasingly more favorable. At small $K = 55$ mN·m/rad for $x > 0$, although the roll mode was more favorable (Fig. 5, *ii*), kinetic energy fluctuation was smaller than the transition barrier (Fig. 4 *C*, *ii*); thus, transition did not occur (Fig. 4 *A*, *ii*). We emphasize that the negative correlation between the probability of staying in or transitioning to a mode and its relative basin height is only an emergent outcome of the transition physics. The passive robot does not directly feel how high or how low an adjacent basin is; whether it escapes and makes a transition only depends on the basin in which it currently resides. Exactly how favorability difference between basins emerges from the local dynamics of escaping from a basin remains to be understood.

Similar to the feedforward-controlled robot, the animal's system state during the observed pitch or roll mode was attracted to the corresponding basin of the potential energy landscape (Fig. 6*A*, ~90% of trials at all K; Movie S10, *Top* and *Middle*). In addition, pitch-to-roll transition mostly occurred when both average kinetic energy fluctuation became comparable to transition barrier and the roll mode became more favorable than the pitch mode (Fig. 6*B* and Movie S10, *Bottom*). These similar observations were remarkable because, for the animal that displayed larger lateral motion and yawing, leg motion, and individual variation, the landscape (which was averaged from all trials) provided a much coarser approximation of the system than for the simpler, well-controlled robot. These animal results supported our first and second hypotheses. We did not test the third hypothesis in the animal, considering that the measured system state velocity was noisy and the animal had higher lateral and yaw motion during traversal.

These results showed that physical interaction with the terrain also played a major role in the animal's probabilistic locomotor transitions, although active behavior was likely at play. In some trials, the animal transitioned even when its average kinetic energy fluctuation was smaller than transition barrier (Fig. 6*B*). In addition, the animal occasionally transitioned to the less favorable roll mode at low K (Fig. 6 *A*, *i* and *ii*, red trajectories). Furthermore, the animal often flexed its head relative to the body and used the two hindlegs differentially (43) during beam interaction (23%, 63%, 89%, 79%, and 85% of the trials at the five K values). All of these were evidence that the animal's transition involved active behavior (see *Discussion*). Unlike the robot that was pulled forward at a constant speed (pulling force always exceeded beam resistive force), the animal had a finite ability to push forward and may rely more on such active behavior to facilitate transition (43).

Discussion

In summary, using a transition between two representative modes in a model system, we demonstrated that an energy landscape approach helps understand how stochastic transitions of animals and robots across locomotor modes statistically emerge from physical interaction with complex 3D terrain. We discovered that kinetic energy fluctuation from oscillatory self-propulsion helps the system cross barriers on a potential energy landscape to make locomotor transitions. This provided compelling evidence about why variation in movement can lead to stochastic outcome (44) and can be advantageous when locomotor behavior is separated into distinct modes. This also explained early observations of the surprising ability to traverse unstructured terrain of bandwidth-limited, rapid-running insects (27) and feedforward-controlled legged robots (45), as both have substantial body oscillation during locomotion. However, we view this way of "vibrate like a particle" as only one of a suite of transition strategies. Animals and robots may use other strategies to make transitions, such as plan anticipatory actions (46), and use random search (47) to overcome barriers, use sensory feedback adjustments to move toward lower barriers or reduce barriers (43), or even change morphology to modify landscape topology to introduce or eliminate certain modes (39).

We posit that there is an "energy landscape-dominated" regime of locomotion, where along certain directions there exist

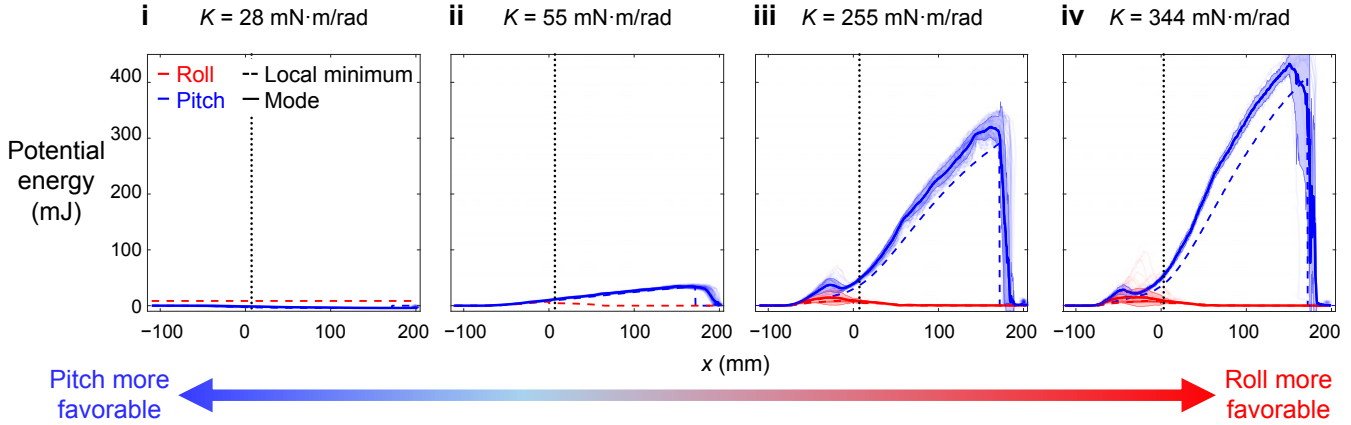

Fig. 5. Favorability measure for robot. Potential energy of measured pitch and roll modes (solid, mean ± SD) and of pitch and roll local minima (dashed) as a function of x. Measured data are for all f tested ($n = 70$ trials) at each K. Blue and red show trials trapped in pitch basin and transitioning to roll basin, respectively. Columns *i*–*iv* are at $K = 28$, 55, 255, and 344 mN·m/rad. The dotted line at $x = 8$ mm shows location of snapshots in Fig. 4*A*. Note that At $K = 28$ mN·m/rad, roll local minimum does not exist. For comparison with other K, we defined it to be at (pitch, roll) = (0°, ±42°) based on the minimal body roll required to traverse without beam deflection.

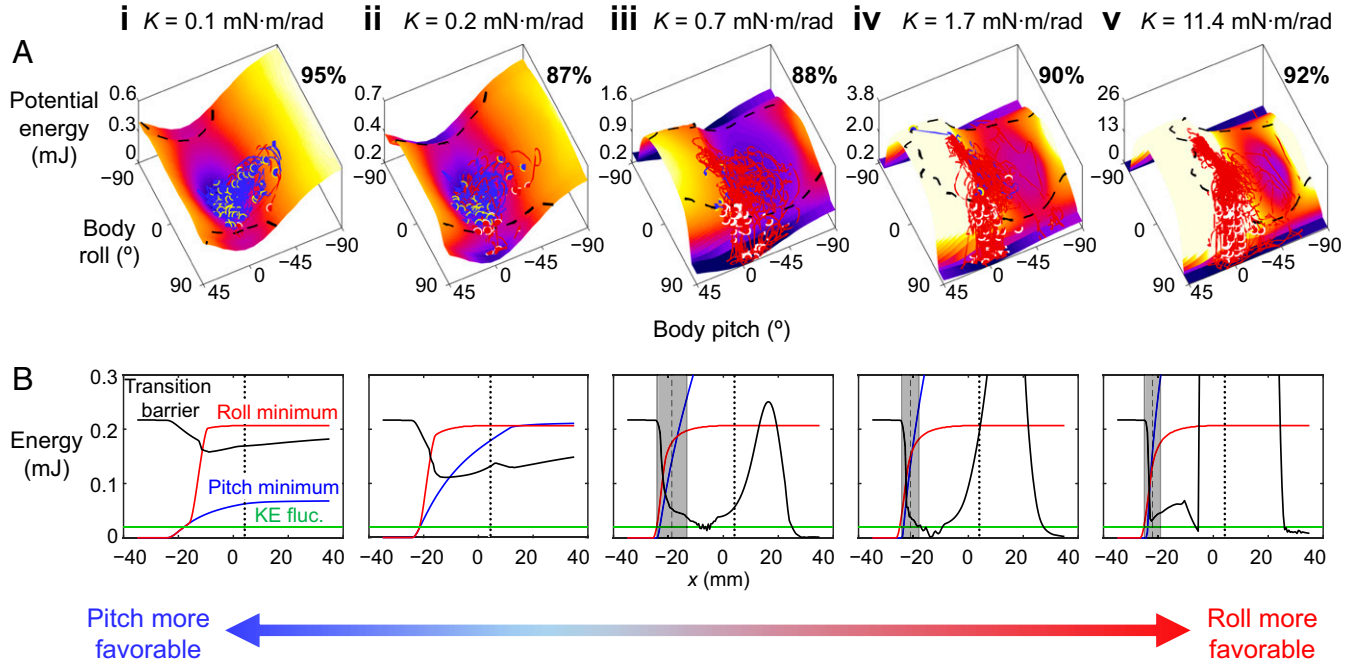

Fig. 6. Animal tends to transition to roll basin when kinetic energy fluctuation is comparable to potential energy barrier to escape pitch basin and when roll basin is more favorable. (*A*) Potential energy landscape over pitch–roll space (snapshot at $x = 4$ mm; dotted lines in *B*) with ensemble of state trajectories. The dashed black curves on landscape show boundary of pitch basin. Note that landscape evolves as body moves forward (increasing x) (Movie S10), and only part of landscape over pitch–roll space is shown to focus on pitch and roll basins. We set color map scale to saturate at high energy to highlight landscape basins. (*B*) Potential energy of pitch and roll local minima and pitch-to-roll transition barrier as a function of x. The green line is measured average kinetic energy fluctuation of 0.02 mJ. Columns *i*–*v* are at $K = 0.1$, 0.2, 0.7, 1.7, and 11.4 mN·m/rad ($n = 64$, 60, 60, 62, and 64 trials).

large potential energy barriers that are comparable to or exceed kinetic energy and/or mechanical work generated by each propulsive cycle or motion. This may happen when propulsive forces are either limited by physiological, morphological, and environmental (e.g., low friction) constraints or do not well align with directions along which large barriers occur. In complex terrain with many large obstacles (34, 39, 43, 46) and even during strenuous maneuvers (35, 47–49), these situations are frequent. In this regime, not only does energy landscape modeling provide a useful statistical physics approach for understanding locomotor transitions across modes, but it may also allow comparison across systems (different animal species, robots, terrain, and modes) to discover general physical principles. Outside of this regime, energy landscape modeling is not useful—for example, not for ballistic jumping over small obstacles with kinetic energy far exceeding potential energy barriers.

We discovered that distinct attractive basins of the potential energy landscape can lead to stereotyped locomotor modes and transitions in both the animal and feedforward-controlled robot. Because our potential energy landscape is directly derived from first principles [as opposed to fitting a model to behavioral data (50–52)], this result provided compelling evidence that behavioral stereotypy of animals emerges from their neural and mechanical systems directly interacting with the physical environment (15, 16). In addition, our approach should inform how direct physical interaction with the environment constrains behavioral hierarchy (15, 16). For example, for grass-like obstacle traversal, starting with our coarse-grained landscape here resulting from a rigid body interacting with rigid "beams" on torsional springs, we can add degrees of freedom describing head flexion (43), body bending and twisting, articulated leg motions, and more realistic beam obstacles with cantilever bending and spatial heterogeneity. This will reveal more nuanced pathways of transitioning between fine-grained locomotor modes that have a variety of body and appendage configuration and terrain responses [e.g., flexing the head and tucking the legs to roll into the gap (43), separating beams laterally, etc.]. Analyzing the disconnectivity (38) of basins of such a more complete, high-dimensional energy landscape will reveal the hierarchy ["treeness" (53)] of locomotor modes in complex terrain.

More broadly, these considerations suggest that our energy landscape approach provides a means toward first-principle, physical understanding of the organization of locomotor behavior, filling a critical knowledge gap. The field of movement ecology (17) makes field observations of trajectories of animals as a point mass moving and making behavioral transitions in natural environments (e.g., ref. 54), whose physical interactions are difficult to measure. Recent progress in quantitative ethology has advanced understanding of the organization of behavior (15, 16, 51–53), often by quantifying kinematics in homogeneous, near featureless laboratory environments (50, 51, 53, 55). Our work highlights the importance and feasibility of, and opens avenues for, studying how the organization of behavior is constrained by an animal's direct physical interaction with realistic environments (24). Doing so will help inform how animal behavior evolves in nature; it will also simplify robot design, control, and planning to generate robust locomotor transitions in complex terrain, which may be otherwise intractable in the large locomotor-terrain parameter space. This is analogous to rugged free energy landscapes allowing divide-and-conquer in protein folding (56).

Our empirically discovered physical principles of locomotor transitions are surprisingly similar to those of microscopic systems (*SI Appendix*, Fig. S7), especially multipathway protein folding transitions where predictive energy landscape theories have been very successful (36–38). Thus, we envision our energy landscape as the beginning of a statistical physics theory that will quantitatively predict global structures and emergent dynamics of multipathway locomotor transitions in the energy landscape-dominated regime.

An immediate next step toward this is to model conservative forces using potential energy landscape gradients and add stochastic, nonconservative propulsive and dissipative forces that perturb the system to "diffuse" across landscape barriers (analogous to refs. 57 and 58). Doing this will also elucidate how escape dynamics from a basin locally leads to emergent favorability difference between basins. These physical principles will help reveal how animals, and how robots should, use local force sensing to control motion to facilitate locomotor transitions on the landscape. Furthermore, although it seems obvious that near-equilibrium statistical thermodynamics does not directly apply here, an energy landscape approach to locomotor transitions in complex terrain provides opportunities to test and develop new theories of few-body active matter (59).

Finally, our energy landscape approach provides a conceptual way of thinking about locomotor modes beyond near–steady-state, limit-cycle–like behavior [e.g., walk, run, climb (6–8)] by adding metastable behavior (60) locally attracted to landscape basins (e.g., pitch and roll modes here, which are far-from-steady maneuvers). We foresee the creation of new dynamical systems theories of terrestrial locomotion (25) that produce transitions across locally attractive landscape basins as well as between limit-cycle attractors (41, 61). They will enable using physical interaction to design, control, and plan basins funneled into one another to compose (62) locomotor transitions to perform high-level tasks in the real world. Terradynamics of locomotor-terrain interaction starting from first principles (24) such as illustrated here will facilitate this progress.

Methods

Robot Experiments. We used a linear actuator to propel the body forward at a constant speed of 0.7 $cm{\cdot}s^{-1}$ and a pair of DC motors via a linkage to vertically oscillate it at a variable frequency f of 0 to 6 Hz and collected a total of 280 trials. We varied K of the beams by using different combinations of torsional springs in parallel.

Animal Experiments. We challenged the discoid cockroach to traverse a layer of beam obstacles. We tested six individuals and beams of the five different K and collected a total of 310 trials.

Potential Energy Landscape Model. We calculated system potential energy as the sum of body and beam gravitational potential energy and beam elastic potential energy:

$$E = m_{\text{body}} g \Delta z + \frac{1}{2} m_{\text{beam}} g L(\cos\Delta\theta_1 + \cos\Delta\theta_2 - 2) + \frac{1}{2} K(\Delta\theta_1^2 + \Delta\theta_2^2), \quad [1]$$

where m_{body} is body mass, g is gravitational acceleration, Δz is body center of mass height increase from its equilibrium configuration (at near zero pitch and zero roll), m_{beam} is beam mass, L is beam length, K is beam torsional stiffness, and $\Delta\theta_1$ and $\Delta\theta_2$ are beam deflection angles from vertical. See *SI Appendix*, Fig. S6 for definition of variables and parameters.

See *SI Appendix, Supplementary Methods* for detailed methods.

Data Availability. All data are included in the main text or *SI Appendix*.

ACKNOWLEDGMENTS. C.L. is grateful to Dan Goldman and Bob Full for early discussion that inspired this study. We are especially grateful to reviewer 2 who nudged us to think more deeply about the broader implications of our work. We thank Qihan Xuan for many insightful discussions, comments on the manuscript, and early preliminary modeling. We thank Dan Koditschek, Bob Full, Dan Goldman, Simon Sponberg, Shai Revzen, Noah Cowan, and two anonymous reviewers for helpful suggestions; reviewer 1 for providing torsional stiffness data of natural flexible terrain elements; Yucheng Kang, Siyuan Yu, and Jundong Yi for help with experimental setup; Yuanfeng Han and Sean Gart for help with animal care; Changxin Yan for verifying tracking accuracy; Yuanfeng Han for characterizing lens distortion; and Yaqing Wang for CAD schematic of animal locomotion arena and counting active behavior in animal trials. This work is funded by an Army Research Office Young Investigator Program (Grant W911NF-17-1-0346), a Burroughs Wellcome Fund Career Award at the Scientific Interface, an Arnold and Mabel Beckman Foundation Beckman Young Investigator Award, and The Johns Hopkins University Whiting School of Engineering start-up funds to C.L.

1. M. H. Dickinson *et al*., How animals move: An integrative view. *Science* **288**, 100–106 (2000).
2. R. M. Alexander, *Principles of Animal Locomotion*, (Princeton University Press, 2006).
3. A. A. Biewener, *Animal Locomotion*, (Oxford University Press, 2003).
4. R. J. Lock, S. C. Burgess, R. Vaidyanathan, Multi-modal locomotion: From animal to application. *Bioinspir. Biomim.* **9**, 11001 (2014).
5. K. H. Low, T. Hu, S. Mohammed, J. Tangorra, M. Kovac, Perspectives on biologically inspired hybrid and multi-modal locomotion. *Bioinspir. Biomim.* **10**, 20301 (2015).
6. R. Blickhan, R. J. Full, Similarity in multilegged locomotion: Bouncing like a monopode. *J. Comp. Physiol. A* **173**, 509–517 (1993).
7. A. D. Kuo, The six determinants of gait and the inverted pendulum analogy: A dynamic walking perspective. *Hum. Mov. Sci.* **26**, 617–656 (2007).
8. D. I. Goldman, T. S. Chen, D. M. Dudek, R. J. Full, Dynamics of rapid vertical climbing in cockroaches reveals a template. *J. Exp. Biol.* **209**, 2990–3000 (2006).
9. D. L. Hu, J. Nirody, T. Scott, M. J. Shelley, The mechanics of slithering locomotion. *Proc. Natl. Acad. Sci. U.S.A.* **106**, 10081–10085 (2009).
10. C. Li, S. T. Hsieh, D. I. Goldman, Multi-functional foot use during running in the zebra-tailed lizard (*Callisaurus draconoides*). *J. Exp. Biol.* **215**, 3293–3308 (2012).
11. A. A. Biewener, M. A. Daley, Unsteady locomotion: Integrating muscle function with whole body dynamics and neuromuscular control. *J. Exp. Biol.* **210**, 2949–2960 (2007).
12. S. Revzen, S. A. Burden, T. Y. Moore, J. M. Mongeau, R. J. Full, Instantaneous kinematic phase reflects neuromechanical response to lateral perturbations of running cockroaches. *Biol. Cybern.* **107**, 179–200 (2013).
13. A. V. Birn-Jeffery *et al*., Don't break a leg: Running birds from quail to ostrich prioritise leg safety and economy on uneven terrain. *J. Exp. Biol.* **217**, 3786–3796 (2014).
14. E. Couzin-Fuchs, T. Kiemel, O. Gal, A. Ayali, P. Holmes, Intersegmental coupling and recovery from perturbations in freely running cockroaches. *J. Exp. Biol.* **218**, 285–297 (2015).
15. G. J. Berman, Measuring behavior across scales. *BMC Biol.* **16**, 23 (2018).
16. A. E. X. Brown, B. de Bivort, Ethology as a physical science. *Nat. Phys.* **14**, 653–657 (2018).
17. R. Nathan *et al*., A movement ecology paradigm for unifying organismal movement research. *Proc. Natl. Acad. Sci. U.S.A.* **105**, 19052–19059 (2008).
18. A. J. Ijspeert, Central pattern generators for locomotion control in animals and robots: A review. *Neural Netw.* **21**, 642–653 (2008).
19. B. Blaesing, H. Cruse, Stick insect locomotion in a complex environment: Climbing over large gaps. *J. Exp. Biol.* **207**, 1273–1286 (2004).
20. T. Kohlsdorf, A. A. Biewener, Negotiating obstacles: Running kinematics of the lizard *Sceloporus malachiticus*. *J. Zool.* **270**, 359–371 (2006).
21. R. E. Ritzmann *et al*., Deciding which way to go: How do insects alter movements to negotiate barriers? *Front. Neurosci.* **6**, 97 (2012).
22. E. L. C. Shepard *et al*., Energy landscapes shape animal movement ecology. *Am. Nat.* **182**, 298–312 (2013).
23. D. M. Bramble, D. E. Lieberman, Endurance running and the evolution of *Homo*. *Nature* **432**, 345–352 (2004).
24. C. Li, T. Zhang, D. I. Goldman, A terradynamics of legged locomotion on granular media. *Science* **339**, 1408–1412 (2013).
25. P. Holmes, R. J. Full, D. Koditschek, J. Guckenheimer, The dynamics of legged locomotion: Models, analyses, and challenges. *SIAM Rev.* **48**, 207–304 (2006).
26. J. C. Spagna, D. I. Goldman, P.-C. Lin, D. E. Koditschek, R. J. Full, Distributed mechanical feedback in arthropods and robots simplifies control of rapid running on challenging terrain. *Bioinspir. Biomim.* **2**, 9–18 (2007).
27. S. Sponberg, R. J. Full, Neuromechanical response of musculo-skeletal structures in cockroaches during rapid running on rough terrain. *J. Exp. Biol.* **211**, 433–446 (2008).
28. J. J. Gibson, "The theory of affordances" in *The Ecological Approach to Visual Perception*, (Psychology Press, 2014), pp. 41–64.
29. S. F. Roberts, D. E. Koditschek, L. J. Miracchi, Examples of Gibsonian affordances in legged robotics research using an empirical, generative framework. *Front. Neurorobot.* **14**, 12 (2020).
30. S. Thrun, Toward robotic cars. *Commun. ACM* **53**, 99 (2010).
31. J.-C. Latombe, *Robot Motion Planning*, (Springer Science and Business Media, 2012).
32. W. Hu, G. Z. Lum, M. Mastrangeli, M. Sitti, Small-scale soft-bodied robot with multimodal locomotion. *Nature* **554**, 81–85 (2018).
33. E. Guizzo, E. Ackerman, The hard lessons of DARPA's robotics challenge. *IEEE Spectr.* **52**, 11–13 (2015).
34. C. Li *et al*., Terradynamically streamlined shapes in animals and robots enhance traversability through densely cluttered terrain. *Bioinspir. Biomim.* **10**, 46003 (2015).
35. C. Li, T. Wöhrl, H. K. Lam, R. J. Full, Cockroaches use diverse strategies to self-right on the ground. *J. Exp. Biol.* **222**, jeb186080 (2019).
36. J. N. Onuchic, P. G. Wolynes, Theory of protein folding. *Curr. Opin. Struct. Biol.* **14**, 70–75 (2004).
37. K. A. Dill, S. B. Ozkan, M. S. Shell, T. R. Weikl, The protein folding problem. *Annu. Rev. Biophys.* **37**, 289–316 (2008).
38. D. J. Wales, *Energy Landscapes: Applications to Clusters, Biomolecules and Glasses*, (Cambridge University Press, 2003).
39. Y. Han, Z. Wang, C. Li, "Body shape helps legged robots climb and turn in complex 3-D terrains" in APS March Meeting 2017. *Bull. Am. Phys. Soc.* **62**, Y12.00002 (2017).

40. J. Aguilar *et al*., A review on locomotion robophysics: The study of movement at the intersection of robotics, soft matter and dynamical systems. *Rep. Prog. Phys.* **79**, 110001 (2016).
41. F. J. Diedrich, W. H. Warren Jr., Why change gaits? Dynamics of the walk-run transition. *J. Exp. Psychol. Hum. Percept. Perform.* **21**, 183–202 (1995).
42. J. A. S. Kelso, Multistability and metastability: Understanding dynamic coordination in the brain. *Philos. Trans. R. Soc. Lond. B Biol. Sci.* **367**, 906–918 (2012).
43. Y. Wang, R. Othayoth, C. Li, "Active adjustments help cockroaches traverse obstacles by lowering potential energy barrier" in APS March Meeting 2020. *Bull. Am. Phys. Soc.* **65**, S22.00003 (2020).
44. G. J. Stephens, M. Bueno de Mesquita, W. S. Ryu, W. Bialek, Emergence of long timescales and stereotyped behaviors in *Caenorhabditis elegans*. *Proc. Natl. Acad. Sci. U.S.A.* **108**, 7286–7289 (2011).
45. R. Altendorfer *et al*., RHex: A biologically inspired hexapod runner. *Auton. Robots* **11**, 207–213 (2001).
46. S. W. Gart, C. Li, Body-terrain interaction affects large bump traversal of insects and legged robots. *Bioinspir. Biomim.* **13**, 26005 (2018).
47. Q. Xuan, C. Li, "A template model reveals self-righting mechanism of a winged robot" in APS March Meeting 2020. *Bull. Am. Phys. Soc.* **65**, S22.00004 (2020).
48. R. Othayoth, Q. Xuan, C. Li, "Induced vibrations increase performance of a winged self-righting robot" in APS March Meeting 2017. *Bull. Am. Phys. Soc.* **62**, Y12.00001 (2017).
49. Q. Xuan, R. S. Othayoth Mullankandy, C. Li, "Randomness in appendage oscillations helps a robot self-right" in APS March Meeting 2019. *Bull. Am. Phys. Soc.* **64**, S64.012 (2019).
50. G. J. Stephens, B. Johnson-Kerner, W. Bialek, W. S. Ryu, Dimensionality and dynamics in the behavior of *C. elegans*. *PLoS Comput. Biol.* **4**, e1000028 (2008).
51. D. S. Mearns, J. C. Donovan, A. M. Fernandes, J. L. Semmelhack, H. Baier, Deconstructing hunting behavior reveals a tightly coupled stimulus-response loop. *Curr. Biol.* **30**, 54–69.e9 (2020).
52. A. B. Wiltschko *et al*., Mapping sub-second structure in mouse behavior. *Neuron* **88**, 1121–1135 (2015).
53. G. J. Berman, W. Bialek, J. W. Shaevitz, Predictability and hierarchy in *Drosophila* behavior. *Proc. Natl. Acad. Sci. U.S.A.* **113**, 11943–11948 (2016).
54. J. P. Suraci, M. Clinchy, L. Y. Zanette, C. C. Wilmers, Fear of humans as apex predators has landscape-scale impacts from mountain lions to mice. *Ecol. Lett.* **22**, 1578–1586 (2019).
55. J. Cande *et al*., Optogenetic dissection of descending behavioral control in *Drosophila*. *eLife* **7**, 1–23 (2018).
56. K. A. Dill, J. L. MacCallum, The protein-folding problem, 50 years on. *Science* **338**, 1042–1046 (2012).
57. N. D. Socci, J. N. Onuchic, P. G. Wolynes, Diffusive dynamics of the reaction coordinate for protein folding funnels. *J. Chem. Phys.* **104**, 5860–5868 (1996).
58. J. D. Bryngelson, P. G. Wolynes, Intermediates and barrier crossing in a random energy model (with applications to protein folding). *J. Phys. Chem.* **93**, 6902–6915 (1989).
59. W. Savoie *et al*., A robot made of robots: Emergent transport and control of a smarticle ensemble. *Sci. Robot.* **4**, eaax4316 (2019).
60. K. Byl, R. Tedrake, Metastable walking machines. *Int. J. Robot. Res.* **28**, 1040–1064 (2009).
61. H. Geyer, A. Seyfarth, R. Blickhan, Compliant leg behaviour explains basic dynamics of walking and running. *Proc. Biol. Sci.* **273**, 2861–2867 (2006).
62. R. R. Burridge, A. A. Rizzi, D. E. Koditschek, Sequential composition of dynamically dexterous robot behaviors. *Int. J. Robot. Res.* **18**, 534–555 (1999).